1 **Through-Culm Wall Mechanical Behaviour of Bamboo**

2 Yusuf Akinbade[1], Kent A. Harries[2], Chelsea V. Flower[3], Ian Nettleship[4], Christopher Papadopoulos[5] and
3 Shawn Platt[6]

4

5 **Abstract**
6 Performance of full-culm bamboo structures is dominated by longitudinal splitting behaviour, often
7 exacerbated by connection details. This behaviour is a function of the transverse properties of this highly
8 orthotropic material. Considerable study of the longitudinal properties of bamboo is available in which it
9 is often concluded that bamboo may be considered as a fibre-reinforced composite material and material
10 properties may be assessed using rule-of-mixture methods. Nonetheless, few studies have addressed the
11 transverse properties of the bamboo culm wall, despite these largely governing full-culm behaviour. This
12 study investigated the transverse material property gradient through the culm wall and attempts to connect
13 the mechanical results to physical observations and phenomena. Most importantly, the study demonstrates
14 that the complex transverse behaviour of bamboo does not appear to behave as a classic fibre-reinforced
15 composite material in the direction transverse to the fibres. In this study, five different bamboo species,
16 *Phyllostachys edulis*, *Phyllostachys bambusoides*, *Phyllostachys meyeri*, *Phyllostachys nigra,* and
17 *Bambusa stenostachya* were tested using a modification of the flat-ring flexure test to obtain a measure of
18 the transverse tensile capacity of the bamboo. Microscopy analyses are used to qualitatively describe the
19 culm wall architecture and to quantitatively assess the failure modes through the culm wall thickness.

20

21 **Keywords**
22 bamboo; fibre gradient; fibre volume; material testing; rule of mixtures; splitting

23

24 **1. Introduction**
25 A functionally graded, natural fibre-reinforced material [Ghavami et al 2003], bamboo has evolved in
26 nature to efficiently resist environmental loads. Bamboo has been shown to have mechanical properties
27 comparable to those of conventional building materials and its worldwide availability gives it great
28 potential as an alternative building material. Rapid growth (mature in 3 to 5 years followed by a 2 to 3
29 year harvest cycle), very low fertilizer requirement (typically none) and the ability to replace conventional

[1] PhD candidate, Department of Civil and Environmental Engineering, University of Pittsburgh
[2] Bicentennial Board of Visitors Faculty Fellow and Professor, Department of Civil and Environmental Engineering, University of Pittsburgh; kharries@pitt.edu
[3] Undergraduate Research Fellow, Department of Civil and Environmental Engineering, University of Pittsburgh
[4] Associate Professor, Department of Materials and Mechanical Engineering, University of Pittsburgh
[5] Associate Professor, Department of Civil and Engineering, University of Puerto Rico at Mayaguez
[6] Post doctoral Researcher, University of Bath, United Kingdom.

30   materials that are resource and energy intensive, combine to make bamboo a potentially sustainable

31   material in terms of both 'carbon footprint' and social equity. Bamboo offers versatility for use in a broad

32   range of international contexts, from use as an affordable and sustainable material in developing countries

33   to rapidly-deployable structures for disaster relief, to mainstream or niche construction in wealthier

34   countries.

35   The structure of bamboo is composed of culms (stalks) with solid transverse diaphragms or 'nodes'

36   separating hollow inter-nodal regions along its height (Figure 1a). The circular cross section (Figures 1b-

37   d) is composed of unidirectional cellulosic fibres oriented parallel to the culm's longitudinal axis

38   embedded in a parenchyma tissue matrix [Grosser and Liese 1971]. The parenchyma tissue matrix

39   lignifies (hardens) as the culm matures leading to increased density and improved mechanical properties.

40   As a functionally graded material, bamboo has evolved to resist its primary loading in nature: its own

41   self-weight and the lateral effects of wind. As seen in Figure 1c, the density of fibres increases from the

42   inner culm wall to the outer culm wall. The wall thickness is largest at the base of the culm and decrease

43   with height up the culm. However, the size and quantity of vessels decrease with the height of the culm

44   and are replaced with bamboo fibres. This addition of fibres compensates for loss in strength and stiffness

45   due to reductions in diameter and wall thickness near the top of the culm, resulting in relatively uniform

46   engineering properties along the entire culm height [Amada 1996; Harries et al. 2017]. Like any fibre-

47   reinforced material, mechanical properties are highly correlated to the proportion and distribution of

48   fibres in the cross section. Mechanical properties are influenced by density, which depends on fibre

49   content, fibre diameter, and cell wall thickness [Janssen 2000]. The density of most bamboo is 700 – 800

50   kg/m^3 depending on species, growing conditions, and position along the culm. The volume fraction of

51   fibres ranges from approximately 60% at the exterior face of the culm wall to 10-15% near the interior

52   face (Figure 1c). The variation in density through the culm wall has been assumed by various researchers

53   to be linear, quadratic, exponential, or a power function and is known to be species-dependent [Amada et

54   al. 1996 and 1997]. Table 1 summarises fibre volume distributions reported in the literature in addition to

55   gross section and inner and outer wall fibre volume ratios (V_f) and longitudinal moduli (E_L). Due to the

56   complex variation of the fibres and vascular bundles, the variation of material properties through the

57   culm-wall thickness has been shown to be significant [Richard and Harries 2015] and to have the effect of

58   increasing gross culm stiffness by about 10% as compared to an assumed uniform distribution of the same

59   volume of fibers [Janssen 2000]. Harries et al. [2017], in a more refined analysis, showed the effect of

60   fibre gradient on gross culm stiffness to result in about a 5% increase for thin-walled culms (D/t < 8) and

61   as much as 20% for thick-walled culms (D/t > 8; where D is the culm outer diameter and t is the culm

62   wall thickness).

63   In general, while highly variable, the longitudinal behaviour of bamboo is relatively well understood in a

64   qualitative sense. From an engineering perspective, the longitudinal behaviour is most typically

65   considered as a fibre-reinforced material in which longitudinal properties are obtained using a rule of

66   mixtures approach. For example, gross section modulus, E_L, is estimated from:

67         $E_L = V_f E_f + (1 - V_f)E_m$ Eq. 1

68   Where V_f is the fibre volume ratio and E_f and E_m are the moduli of the fibre and matrix (parenchyma)

69   phases, respectively. Janssen (2000) reports typical values of $E_f = 35$ GPa and $E_m = 1.8$ GPa.

70   The dominant failure mode of bamboo, however, is longitudinal splitting associated with bamboo

71   carrying flexure, compression or tension loads; splitting is exacerbated by the use of simple bolted

72   connection details common in some bamboo construction [Sharma et al. 2012]. Janssen [1981] describes

73   the bending stresses in a culm as being characterised by the longitudinal compressive stress and

74   transverse strain in the compression zone of the culm, with failure eventually occurring due to

75   longitudinal splitting. This is ideally a Mode II[7] longitudinal shear failure. However, in the presence of

76   perpendicular stresses (as is the case where ever there is a non-zero shear-to-moment ratio), there is some

77   Mode I component stress which significantly reduces the Mode II capacity. Richard et al. [2017]

78   demonstrate the effects of such mode mixity using longitudinal shear tests [ISO 2004] which capture pure

79   Mode II behaviour, split pin tests [Mitch et al. 2010] which capture Mode I behaviour, and culm bending

80   tests of different spans resulting in different degrees of mode mixing. For two different species, a thin

81   walled *P. edulis* and thick-walled *B. stenostachya*, the split pin tests resulted in Mode I capacities equal to

82   only 18% of the Mode II capacity determined from the longitudinal shear tests. Beam tests having mixed

83   mode behaviour exhibited shear capacities ranging from 40-70% of the Mode II capacity.

84   Both the Mode I and II behaviours described are primarily functions of the transverse properties of the

85   fibre-reinforced culm which are believed to be dominated by matrix (parenchyma) properties. Despite

86   their importance in the dominant observed behaviour of full-culm bamboo, there are few studies of the

87   transverse properties of the culm wall. In early work, Arce-Villalobos [1993] concluded that there is no

88   correlation between the density of bamboo and its transverse tensile strength. Janssen [2000], based on

89   flexural tests, reports that a transverse strain of 0.0013 results in transverse tensile failure of the culm wall

90   (with no indication of species or other variation). More recently, test methods have been proposed for

91   obtaining transverse properties of bamboo culms [Mitch et al. 2010; Sharma et al. 2012; Virgo et al.

92   2017] although these have not yet been widely adopted to obtain material properties over a range of

93   species and conditions. Sharma and Harries [2012] report a unique attempt to refine an edge bearing test

94   to determine through culm-wall distribution of properties. In this study, the culm was cut, using a water

---

[7] Reference to Modes II and I are in relation to classical fracture mechanics in which Mode II refers to forces resulting
in 'in-plane shear' and Mode I refers to perpendicular in-plane 'peeling' forces.

95   jet, into two or three concentric annular sections. Edge bearing test results for each resulting 'ring'

96   provided an improved measure of through-thickness transverse properties than could be obtained from a

97   single full-culm section. The approach was limited to thicker culm walls, provided only two or three data

98   points across the culm wall and did not result in repeatable specimens and was therefore abandoned.

99   Tan et al. [2011] conducted a micro-scale study on the crack growth and toughening mechanisms of *P.*

100   *edulis*. The study revealed that toughening was inversely related to fibre density. The authors noted that

101   their results suggest the need to account for the anisotropic strength and fracture properties of bamboo in

102   the design of bamboo structures.

103   In order to understand the transverse behaviour of bamboo, it is informative to consider laminate theory

104   and the rule of mixtures for transverse properties:

105        $E_T = [V_f/E_f + (1 - V_f)/E_m]^{-1}$ Eq. 2

106   Equation 2 is conventionally considered a lower-bound estimate of transverse properties since it does not

107   account for the anisotropic nature of the fibre itself and, as a result, underestimates off-longitudinal

108   properties [Mallick 2008]. The Halpin-Tsai equations [Halpin and Kadros 1976] are most often adopted

109   to describe transverse behaviour of fibre-reinforced composites:

110        $E_T = E_m(1 + \xi n V_f)/(1 - n V_f)$ Eq. 3

111   Where $n = (E_f/E_m - 1)/(E_f/E_m + \xi)$ Eq. 4

112   The value of ξ is an empirical constant fitted to the elasticity solution for a fibre geometry and confirmed

113   by experimental data [Halpin and Kadros 1976]:

114        $\xi = 2 + 40V_f^{10}$ Eq. 5

115   When considering transverse properties of longitudinally reinforced fibre composites having V_f less than

116   0.5, it is conventional to assign $\xi = 2$ [Hewitt and de Malherbe 1970]. Halpin-Tsai is equally applicable to

117   determining longitudinal properties. For longitudinal properties of long continuous fibre composites (such

118   as bamboo) however, Halpin-Tsai results in the same relationship as the rule-of-mixtures (Eq. 1).

119   Figure 2 presents theoretical longitudinal and transverse modulus distributions determined using the rule

120   of mixtures and Halpin-Tsai, respectively (Equations 1 and 3). The fibre volume distribution illustrated is

121   that proposed by Dixon and Gibson [2014] for *P. edulis* and is representative of most distributions

122   reported in Table 1. The modulus distributions shown are normalised by the average modulus for the

123   culm wall which is what should be obtained when testing a full-culm specimen (i.e., the apparent modulus

124   of the gross section). In addition to the variation in properties, a shift of the neutral axis of the section (at

125   which location ratios equal unity) toward the outer culm wall is evident. This shift results in the increase

126   in gross culm stiffness described previously [Janssen 2000; Harries et al. 2017].

127   The objective of the present study is to investigate the transverse material property gradient through the

128   culm wall and to connect the mechanical results to physical results, such as fibre density. In this study, a

129   modification to the flat-ring flexure [Virgo et al. 2017] test specimen, in which only portions of the culm

130   wall cross-section are tested, is used to obtain a measure of the transverse tensile capacity of the bamboo.

131   Microscopy analyses are used to qualitatively describe the culm wall architecture and to quantitatively

132   assess the failure modes through the culm wall thickness. Throughout this study, all data is also

133   normalised by culm wall thickness ($x = 0$ is the inner wall and $x = 1$ is the outer wall).

134   **2. Flat-ring Flexure Test**

135   The flat ring flexure test [Virgo et al. 2017] assesses the tendency of bamboo to fail via longitudinal

136   cracks using a full cross-sectional specimen that is $L \approx 0.2D$ in length. The specimen is subjected to 4-

137   point flexure as shown in Figure 3. The desired failure for this test occurs in the constant moment region.

138   The flat ring flexure test gives the apparent modulus of rupture of the specimen (f_r) which, due to

139   specimen geometry, is related to the transverse tension capacity of the bamboo. The modulus of rupture is

140   calculated from the test results as:

141             $f_r = 3Pa/(t_N + t_S)L^2$ Eq. 5

142   Where P is total load applied to specimen; a is the shear span; t_N and t_S are culm wall thickness at the

143   failure locations on either side of the culm; and L is the length of culm section tested (i.e., the flexural

144   depth of specimen). A practical test span is found to be approximately $S = 0.85D$ and the shear span

145   should be at least $0.33S$. This test is easily translated to a field setting, requiring only two loading plates,

146   four pins, and free weights, rather than a hydraulic press. Nonetheless, in this study, all tests were carried

147   out in a mechanically driven universal test machine. Tests are conducted in displacement control at a rate

148   of crosshead travel of 0.76 mm/min resulting in failure in between 1 and 5 minutes. Loads are obtained

149   using a load cell with a precision of ± 0.4N. A specimen loading apparatus (Figure 3b) is used to ensure

150   accurate and repeatable specimen alignment. With this apparatus, test span and shear span can be varied

151   independently in increments of 5 mm. Prior to this study, the flat-ring flexure test has been used on only

152   full-culm cross sections. Such full-culm cross section specimens are referred to in this work as the control

153   specimens and the modulus of rupture thus obtained is denoted f_{rC}.

154   **2.1 Clipped Flat-ring Test Specimens**

155   This study adopts a modification to the flat-ring test specimen, in which only portions of the cross-section

156   are tested in order to determine the effect of the material property gradient through the culm wall. The

157   culms were cut into full cross-section specimens approximately $0.2D$ in length. Approximately 20

158   specimens were obtained from each internode and all specimens are obtained from three or four adjacent

159   internodes. In this way it can reasonably be assumed that there is little variation in properties among

160   specimens. Importantly, there is little variation in D and t among the samples used. 'Clipped' specimens

161   (Figure 4a) had test regions machined using an end mill (Figure 4b). Specimens were machined such that

162     $\alpha \approx 0.20t$ or $0.25t$ and β and γ are in increments of approximately $0.20t$ or $0.25t$ such that the sum $\alpha + \beta +$

163    $\gamma = t$, the culm wall thickness. This approach divides the culm wall into segments for which the modulus

164   of rupture determined from each segment is calculated from Eq. 6 and is assumed to represent the average

165   value for that segment; the value is then assigned to the centroid of the segment.

166        $f_r = 3Pa/(\alpha t_N + \alpha t_S)L^2$ Eq. 6

167   The machining was controlled such that α and β at both the N and S quadrant are the same in each

168   specimen (as a result, γ may differ slightly based on variation of t in the cross section). All as-tested

169   dimensions were recorded and these are used in individual calculations of specimen capacity. Control

170   specimens were not clipped; thus $\alpha = t$ and $\beta = \gamma = 0$. The results from the control specimens represent the

171   gross cross-section modulus, f_{rC}, against which the clipped-specimen data is normalised.

172   **3. Specimen Materials**

173   Five different bamboo species were tested in this study, *Phyllostachys edulis*, *Phyllostachys bambusoides*,

174   *Phyllostachys meyeri*, *Phyllostachys nigra,* and *Bambusa stenostachya*. All are thin-walled (*D/t* generally

175   greater than 8) except *B. stenostachya* which is a thick-walled species. All *Phyllostachys* culms were

176   obtained from a commercial importer and were water treated and kiln dried. The *B. stenostachya* was

177   commercially imported from Vietnam and was borax treated.

178   In order to place the materials reported in this study in the context of the broader literature, standard

179   longitudinal compression and longitudinal shear (so-called "bow-tie" test) tests (ISO 22157:2019) of all

180   species were conducted; the results are reported in Table 2. Bamboo density normalized for 12%

181   moisture content, ρ_{12}, (ISO 22157:2019) is also reported in Table 2. Specimens had been stored in a

182   laboratory environment for some time prior to testing; the moisture content of all specimens at time of

183   testing was between 13% and 15% as measured with an electronic (pin-type) moisture meter (Table 2).

184   The objective of this study is to assess the effects of through-culm wall fibre distribution. In order to limit

185   – to the extent possible – material variation, all specimens reported in this paper were taken from the

186   lower region of only a few culms coming from the same batch of each species. Test specimens were cut

187   from within 2 m of each other and included 0.2*D* long specimens for flat ring flexure and 1.0*D* long

188   specimens for compression and longitudinal shear testing. Adjacent samples were used for control and

189   clipped specimens. At least 30 control specimens were tested for each species and as many as 6

190   specimens of each clipped case were tested (*n* in Tables 3 and 4). Average culm diameter, *D*, and wall

191   thickness, *t*, for each group of samples are reported with the summary of test results in Tables 3 and 4.

192   **3.1 Fibre Distribution**

193   Seven full-culm cross sections (four for *B. Stensostachya*) were selected and digital images were taken at

194   each of the four quadrants (N, S, E and W). These images were processed using a purpose-built MatLab

195   script to obtain the distribution of fibres through the wall cross section. An example of a collected image

196   and resulting MatLab pixel map is shown in Figure 5. The collected images are square, having a

197   dimension equal to the culm-wall thickness, t (Figure 5a). The image is divided in the through-thickness

198   direction into ten equal regions of thickness $t/10$ (Figure 5b) and the fibre volume ratio obtained for each

199   (Figure 5c). From this analysis, the average fibre distribution (expressed as third-order polynomial best-

200   fit curves) is obtained as summarised at the bottom of Table 1 in terms of the normalised culm wall

201   thickness, x ($x = 0$ is the inner culm wall and $x = 1$ is the outer culm wall). The coefficient of variation of

202   measured fibre volume ratios was less than 0.18 for all but *P. nigra*, which exhibited a COV = 0.24. The

203   28 *P. edulis* samples shown in Figure 5c have a COV = 0.13. The best-fit equations representing fibre

204   volume distribution reported in Table 1 all have a coefficient of determination $R^2 = 0.99$.

205   The fibre distribution among the four thin-wall *Phyllostachys* species is very similar. Indeed, a single

206   relationship could be given for all four species having $R^2 = 0.96$ as shown in Table 1. A marked

207   difference in fibre distribution is observed in the thick-walled *B. stenostachya*. Thus, fibre distribution is

208   observed to differ by genera (*Phyllostachys* and *Bambusa*) but less so among species in the same genera

209   (*Phyllostachys*).

210   **4. Full-wall Thickness Flat-Ring Flexure Test Results**

211   Modulus of rupture, f_{rC}, (Eq. 5) determined for the full-culm control specimens is reported in Table 3.

212   Within the genus *Phyllostachys*, these values are similar and notably greater than that observed for *B.*

213   *stenostachya*. Observed variation of test results is typical of bamboo and similar to that reported in Virgo

214   et al. [2017]. As recommended by Virgo et al., only specimens failing within the constant moment region

215   (Figure 3a) are included in the reported data. Additionally, outliers defined as data falling outside 1.5

216   times the interquartile range (so called Tukey fences (Hoaglin 2003)), were excluded from the reported

217   data.

218   **5. Clipped Flat-ring Test Results**

219   Experimentally determined values of normalised f_r/f_{rC} determined from the clipped tests are shown in

220   Figure 6 and the corresponding best fit second-order polynomial relationships are reported in Table 3.

221   These all illustrate a similar trend although *P. nigra* specimens exhibit relatively little variation through

222   the culm wall compared to the other species. With the clipped specimens, all failures occurred in the

223   clipped region and no data was determined to be an outlier.

224   **6. Effect of Outer Layer of Bamboo Culm**

225   Integrating the f_r/f_{rC} best-fit curves (Table 3) from $x = 0$ to $x = 1$ should represent the gross modulus

226   across the section; that is, the integral $\int f_r/f_{rC} dx$ should equal unity. However, as shown in Table 3, with the

227   exception of *P. meyeri*, the gross modulus obtained by integrating the clipped data exceeds unity by as

228   much as 20%. A possible explanation for this behaviour – one in which the sum of the parts exceeds the

229   capacity of the whole – is that failure of the full wall section control specimens is being initiated by a

230 'weak link'. A brittle failure of the outer layer of the culm wall initiating failure would explain this

231 observation.

232 The extreme outer layer of a bamboo culm consists of a silica-rich outer skin (epidermis) and a thin

233 region of densely packed fibres (this can be seen at the top of Figure 5). It is believed that this layer will

234 be more brittle than the rest of the culm wall and may help to initiate failures in specimens in which the

235 outer wall is included. Therefore in the clipped specimen testing a question arises: *is the outer layer*

236 *contributing disproportionately to the observed behaviour, especially to the control and β = 0 tests*? To

237 investigate this effect, additional specimens were tested having $\beta \approx 0.05t$ and $\alpha \approx 0.95t$ (i.e. $\gamma = 0$, see

238 Figure 4a); essentially, these are full-culm sections with only the outer layer 'shaved' away.

239 Twenty flat-ring flexure specimens were cut from comparable samples of each species tested in the

240 clipped test program (*P. edulis* was not included as there were no comparable specimens available).

241 Alternating specimens along the culm were prepared using a belt sander such that $\beta \approx 0.05t$ and $\alpha \approx 0.95t$

242 (Figure 4a). Resulting wall thicknesses in the constant moment region are reported in Table 4. Apart from

243 specimen preparation, all tests were identical to those reported previously. To assess potential changes in

244 specimen ductility, displacement of the applied load, δ, was measured and reported at failure of each

245 specimen. Results are presented in Table 4. Also shown in Table 4 is the p-value determined from an

246 unpaired t-test for each set of 'shaved' and unshaved specimen. The p-value is the probability that there is

247 no statistically significant difference between the compared conditions.

248 It is seen that the modulus of rupture, f_r, is essentially unaffected by the removal of the outer layer. With

249 the exception of *P. nigra,* the displacement at failure is observed to increase upon the removal of the outer

250 layer. This increase is greater than can be attributed to the loss of 5% of the moment of inertia of the cross

251 section (resulting from shaving the specimen) alone. To consider the observed behaviour in a normalised

252 fashion, the tangent 'stiffness', f_r/δ is also calculated. As seen in Figure 7, specimen stiffness (represented

253 as linear best-fit line in Figure 7) falls on the order of 15 to 30% (with the exception of *P. nigra*) despite

254 the moment of inertia being reduced only 5%. The modulus of rupture itself remains unchanged.

255 **7. Discussion of Observed Transverse Behaviour**

256 The data shown in Figure 6 and equations reported in Table 3 indicate a generally parabolic distribution

257 of modulus of rupture through the culm wall thickness with higher values at both the inner and outer

258 walls and a minimum near the middle of the wall thickness. The fibre volume distributions, also shown in

259 Figure 6 and given in Table 1, indicate a typically observed distribution having few fibres at the inner

260 wall and a greater volume fraction at the outer wall. Based on these fibre distributions, the predicted

261 distribution of modulus of rupture using the Halpin-Tsai equation (Equation 3) does not appear to capture

262 the experimentally observed behaviour, particularly in the inner half of the culm wall where fibre volumes

263   are lowest. Bamboo does not appear to be behaving as a classic fibre-reinforced composite material in the

264   direction transverse to the fibres.

265   The observed behaviour requires further study and may represent a material variation or morphological

266   variation through the bamboo culm wall thickness. To investigate this further, the failure planes of full-

267   culm wall thickness control specimens were investigated using a scanning electron microscope (SEM).

268   Figure 8 shows an SEM image of a typical *P. edulis* vascular bundle (near the outer culm wall) showing

269   the fibre bundles comprised of microfibrils surrounding the vessel and the parenchyma into which the

270   bundle is embedded. In Figure 8, the fibre bundle can be seen to be penetrated by intra-fibril cracks

271   whereas the interfaces between fibres and parenchyma appear quite intact. It is noted that the parenchyma

272   cell walls are relatively thick indicating a relatively mature culm age [at harvest] (Liese and Weiner

273   1996). The cracking of the fibres may therefore be a function of culm age (observed although not

274   described by Liese and Weiner). The age at harvest of the bamboo used in this study is unknown and

275   without comparative images, age cannot be estimated. Liese and Weiner (1996), however clearly describe

276   and Liese (1998) illustrates the thickening of the parenchyma wall with age. Alternatively, these cracks

277   may have formed as a result of shrinkage associated with drying (desiccation of the vessel) or treatment

278   of the bamboo. Chen et al (2018) clearly describes different behaviour of the parenchyma and interaction

279   between the parenchyma and fibres based on moisture content. Orsorio et al. (2018) argues that these

280   cracks result for extraction and preparation of the SEM sample. Further study will be made to address the

281   source of these cracks – which are relatively commonly seen – as they represent a stress raiser in the

282   adjacent parenchyma and may be the source of cracks in the parenchyma. Such an effect is shown in an

283   image in Chen et al. (2018) although not described by the authors.

284   Figure 9 shows SEM images taken from the failure plane of a flat-ring flexure test specimen. Each failure

285   plane was divided into a grid and images of each obtained, allowing the entire failure plane to be imaged.

286   The images shown in Figures 9b and 9c are typical of images obtained at the outer and inner walls,

287   respectively, of a *P.edulis* specimen obtained slightly above the neutral axis of the section in flexure (see

288   Figure 9a). Image features did not vary considerably based on their location through the depth of the

289   specimen (dimension L in Figure 9a).

290   In Figures 9b and 9c the failure plane can be seen to both follow the edge of the fibre bundles but also to

291   go through the bundles themselves – presumably propagating along the cracks observed in Figure 8. In

292   some locations, the failure plane can be seen to expose the vessels (voids) surrounded by the bundle.

293   Where it is seen at the failure plane, the interface between the parenchyma and the fibre bundle appears

294   intact. This supports the observation that the cracks in the fibre bundle initiate cracks in the parenchyma.

295   In such a case the failure plane represents the propagating crack and little damage would be expected at

296   interfaces parallel to the crack plane. Similar behaviour is reported by Chen et al. (2018) as the

297   propagation of cracks through the parenchyma but around the mircofibrils comprising the fibre bundle.

298   Additionally, the parenchyma shown in Figures 9b and 9c, appear to be behaving differently. Near the

299   outer culm wall (Figure 9b), the failure appears to follow the interfaces between parenchyma cells. Near

300   the inner culm wall (Figure 9c), the failure plane often appears to pass through the parenchyma cells (seen

301   as non-intact cell walls in Figure 9c). This observation is typical of all images obtained in this study.

302   Indeed, near the outer culm wall, the parenchyma is occasionally observed to fail in 'sheets' of intact cells

303   as shown in Figure 10a. In other images (Figure 10b) the intact parenchyma close to the inner culm wall

304   appear 'desiccated': the intact cell wall appears to be 'caving in' or concave rather than being slightly

305   convex nearer the outer culm wall (Figure 8). This observation may suggest a gradient in moisture content

306   through the culm wall or a residual effect of moisture gradient during the drying process – recall that the

307   *P. edulis* was kiln-dried. Such a gradient should be expected. The bamboo culm epidermis is relatively

308   impermeable and resistant to wetting whereas the inner culm wall is permeable (Liese 1998, Yao et al.

309   2011). The effects of moisture content, 0%, 6% and 20%, on parenchyma behaviour of *P. edulis* has been

310   recently reported by Chen et al. (2018) who attribute increased toughness – particularly of the

311   parenchyma matrix, with increased moisture content.

312   The longitudinal aspect ratio of the parenchyma cells can be seen to be different in the outer (Figure 10a)

313   and inner (Figure 10b) regions of the culm wall. In recent work, Zeng et al. (2019) identified significantly

314   different morphology of parenchyma cell walls through the culm wall thickness of *P. edulis* samples.

315   Near the outer culm wall, parenchyma cell walls were tightly packed laminar structures with little annular

316   space at interstices (Figure 11c). Nearer the inner culm wall, the laminar structure of the cell wall was

317   separating and a larger triangular pore is present at parenchyma cell interstices (Figure 11a). It is unclear

318   how these differences impact the behaviour illustrated in Figure 9 but it is evident that parenchyma is not

319   homogeneous through the cross section. Neither Zeng et al. (2019) nor Liese (1998) provide insight on

320   the source of this inhomogeneity and the present authors can only speculate on its cause, although it does

321   appear to affect the through thickness mechanical behaviour of the culm wall.

322   **8. Conclusion**

323   This study investigated the transverse material property gradient through the bamboo culm wall and

324   attempts to connect the mechanical results to physical observations and phenomena. Most importantly,

325   the study demonstrates that the transverse behaviour is complex and that bamboo does not appear to

326   behave as a classic fibre-reinforced composite material in the direction transverse to the fibres.

327   In this study, a modification to the flat-ring flexure test specimen, in which only portions of the culm wall

328   cross-section are tested, is used to obtain a measure of the transverse tensile capacity of the bamboo.

329 Microscopy analyses are used to qualitatively describe the culm wall architecture and to quantitatively

330 assess the failure modes through the culm wall thickness. The following conclusions are made:

331 1. Fibre volume distribution through the culm wall was best described by third-order polynomial curves

332 and the COV was observed to be on the order of 0.20 in all cases. Fibre distribution and modulus of

333 rupture, f_{rC}, among the four thin-wall *Phyllostachys* species was very similar, while the same values

334 for *B. stenostachya* was markedly different.

335 2. The gross modulus obtained by integrating the clipped data exceeds the experimentally determined

336 value of f_{rC} by as much as 20%; that is, the sum of the parts exceeds the capacity of the whole culm.

337 3. The silica-rich epidermal layer of the culm wall appears to disproportionately affect the full-culm

338 modulus, f_{rC}. Full-culm specimens were tested without this layer and the modulus of rupture was

339 essentially unaffected. The stiffness of the specimens tested without the epidermal layer was reduced

340 considerably more than the small reduction in geometry implies.

341 4. The distribution of fibre volume and modulus of rupture though the culm wall thickness are shown to

342 not be correlated by conventional assumptions of fibre-reinforced composite material behaviour. The

343 Halpin-Tsai equation (Equation 3) does not appear to capture the experimentally observed behaviour,

344 particularly in the inner half of the culm wall where fibre volumes are lowest.

345 Scanning electron microscopy (SEM) images of the flat-ring flexure tests failure surfaces reveal a

346 complex behaviour that is not consistent with the assumptions of fibre-reinforced composite behaviour.

347 The following is observed:

348 5. Failure planes generally pass through the fibre bundles, affected by the vessels (voids) contained in

349 the bundles and cracking between individual fibres comprising the bundles. In general, the interface

350 between fibres and parenchyma (matrix) remains intact.

351 6. Failure within the parenchyma also varies based on location through the culm wall. Near the outer

352 culm wall, the failure appears to follow the interfaces between parenchyma cells however near the

353 inner culm wall, the failure often appears to pass through the parenchyma cells.

354 7. Morphologic characteristics of the parenchyma are seen to vary through the culm wall thickness

355 although it is unclear how these differences impact behaviour.

356 Considerably more research is required to understand the source of the variation in parenchyma structure

357 and its effect on mechanical properties of the bamboo culm. The variation may simply be the natural

358 morphology of the bamboo but may also arise from drying, curing and/or treatment processes. While

359 gross section properties are most important for full-culm bamboo construction, variation of properties

360 through the culm wall may be critical to the performance of laminated bamboo products, particularly

361 those employing tangentially cut strips such as glue-laminated bamboo and cross laminated bamboo

362 [Sharma et al. 2015].

363

References

Amada, S., Ichikawa, T., Munekata, T., Nagase, Y., and Shimizu, H., (1997) Fiber texture and mechanical graded structure of bamboo, *Composites: Part B*, **28B**, 13-20.

Amada, S., Munekata, T., Nagase, Y., Ichikawa, Y., Kirigai, A. and Zhifei, Y. (1996) The mechanical structures of bamboos in viewpoint of functionally gradient and composite materials, *Journal of Composite Materials*, **30**, 800-819.

Arce-Villalobos O.A. (1993) *Fundamentals of the design of bamboo structures*, Master's thesis, Eindhoven University of Technology, The Netherlands.

Chen G., Luo H., Yang H., Zhang, T. and Li, S. (2018) Water effects on the deformation and fracture behaviors of the multi-scaled cellular fibrous bamboo. *Acta Biomaterialia* **65**, 203-215

Dixon, P.G. and Gibson, L.J. (2014) The structure and mechanics of Moso bamboo material, *Journal of the Royal Society Interface* **11**, 20140321.

Dixon, P.G., Ahvenainen, P., Aijazi, A.N., Chen, S.H., Lin, S., Augusciak, P.K., Borrega, M., Svedstrom, K. and Dixon, L.J., Comparison of the structure and flexural properties of Moso, Guadua and Tre Gai bamboo, *Construction and Building Materials*, **90**, 11-17.

Ghavami, K. and Marinho, A.B. (2005) Propriedades físicas e mecânicas do colmo inteiro do bambu da espécie Guadua angustifolia, *Revista Brasileira de Engenharia Agrícola e Ambiental*, **9**(1), 107-114. (in Portuguese)

Ghavami, K., Rodriques, C.S., and Paciornik, S., (2003) Bamboo: Functionally Graded Composite Material, *Asian Journal of Civil Engineering (Building and Housing)*, **4**(1), 1-10.

Grosser and Liese (1971) On the anatomy of Asian Bamboos, with Special Reference to their vascular bundles. *Wood Science and Technology*, **5**, 290-312.

Habibi, M.K., Samaei, A.T., Gheshlaghi, B., Lu, J. and Lu, Y. (2015) Asymmetric flexural behaviour from bamboo's functionally graded hierarchical structure: Underlying mechanisms, *Acta Biomaterialia*, **16**, 178-186.

Halpin, J.C. and Kardos, J.L. (1976) The Halpin-Tsai Equations: A Review, *Polymer Engineering and Science* **16**(5), 344-352.

Harries, K.A., Bumstead, J., Richard, M.J. and Trujillo, D. (2017) Geometric and Material Effects on Bamboo Buckling Behaviour, *ICE Structures and Buildings* Themed issue on bamboo in structures and buildings, **170**(4), 236-249.

Hewitt, R.L. and de Malherbe, M.C. (1970) An Approximation for the Longitudinal Shear Modulus of Continuous Fiber Composites, *Composite Materials*, **4,** 280.

Hoaglin, D.C. (2003) John W. Tukey and Data Analysis*, Statistical Science* **18**(3), 311-318.

ISO 22157:2019 *Bamboo structures -- Determination of physical and mechanical properties of bamboo culms -- Test methods*. International Organization for Standardization

Janssen, J. (1981) *Bamboo in Building Structures*. Doctoral Dissertation, Eindhoven University of Technology, Netherlands.

Janssen, J.J.A., (2000) *Designing and Building with Bamboo*, INBAR Technical Report 20. International Network for Bamboo and Rattan, Beijing, China.

Krause, J.Q., Andrade Silva, F., Ghavami, K., Gomes, O.F.M, Toledo Filho, R.D., On the influence of Dendrocalamus giganteus bamboo microstructure on its mechanical behavior, *Construction and Building Materials*, **127**, 199-209.

414   Liese, W. (1998) *The Anatomy of Bamboo Culms*, Brill. 204 pp.

415   Liese, W. and Weiner, W. (1996) Ageing of Bamboo Culms. A Review. *Wood Science and Technology*,
416   **30**, 77-89.

417   Mallick, P. K. (2008). *Fiber-reinforced composites: materials, manufacturing, and design* (third edition).
418   CRC press.

419   Mitch, D., Harries, K.A., and Sharma, B. (2010) Characterization of Splitting Behavior of Bamboo
420   Culms. *ASCE Journal of Materials in Civil Engineering* **22**, 1195-1199.

421   Nogata, F. and Takahashi, H. (1995) Intelligent functionally graded material: bamboo, *Composites*
422   *Engineering*, **5**, 743-751.

423   Osorio L., Trujillo E., Lens F., Ivens, J. Verpoest, I. and Van Vuure, AW., (2018) In-depth study of the
424   microstructure of bamboo fibres and their relation to the mechanical properties. *Journal of Reinforced*
425   *Plastics and Composites* **37**, 1099-1113

426   Richard, M. (2013) *Assessing the Performance of Bamboo Structural Components*, Doctoral Dissertation,
427   University of Pittsburgh.

428   Richard, M., Gottron, J., Harries, K.A. and Ghavami. K. (2017) Experimental Evaluation of Longitudinal
429   Splitting of Bamboo Flexural Components, *ICE Structures and Buildings* Themed issue on bamboo in
430   structures and buildings, 170(4), 265-274

431   Richard, M.J., Harries, K.A., (2015) On Inherent Bending in Tension Tests of Bamboo, *Wood Science*
432   *and Technology* **49**(1) 99-119.

433   Shao, Z.P., Zhou, L., Liu, Y.M., Wu, Z.M. and Arnauld, C. (2010) Differences in structures and strength
434   between internode and node sections of Moso bamboo, *Journal of Tropical Forest Science*, **22**(2),
435   133-138.

436   Sharma B, Gatoo A, Bock M, Ramage M (2015) Engineered Bamboo for structural applications.
437   *Construction and Building Materials*, **81**, 66-73.

438   Sharma, B., Harries, K.A. and Ghavami, K. (2012) Methods of Determining Transverse Mechanical
439   Properties of Full-Culm Bamboo, *Journal of Construction and Building Materials*, **38**, 627-637.

440   Sharma, B. and Harries, K.A. (2012). Effect of Fiber Gradation on the Edge Bearing Strength on Bamboo
441   Culms, *Key Engineering Materials*, Vol 517, pp 63-70.

442   Tan, T., Rahbar, N., Allameh, S.M., Kwolfie, S., Dissmore, D., Ghavami, K. and Soboyejo, W.O. (2011)
443   Mechanical Properties of functionally graded hierarchical bamboo structures, *Acta Biomaterialia* **7**,
444   3796-3803.

445   Vaessen, M.J. and Janssen, J.A. (1997) Analysis of the critical length of culms of bamboo in four-point
446   bending tests, *HERON*, **42**(2), 113-124.

447   Virgo, J., Moran, R., Harries, K.A., Garcia, J.J., and Platt, S. (2017) Flat Ring Flexure Test for Full-Culm
448   Bamboo, *Proceedings of 17th International Conference on Non-Conventional Materials and*
449   *Technologies (17NOCMAT)*, Yucatán, México, November 2017.

450   Yao, L.H., Wang, X.M. and Fei, B.H. (2011) Study on Permeability Coefficient of Different Bamboo/Fir
451   Veneer Surface, *Advanced Materials Research*, **311-313**, 1634-1637.

452   Zeng, Q., Zhang, Q., Lu, Q., Zhou, Y., Chen, N., Rao, J. and Fan, M. (2019; in press) Wetting behavior
453   and laminate bonding performance of profiled tangential surfaces of moso bamboo, *Industrial Crops*
454   *and Products*

455

Table 1 Summary of through-culm wall fibre volume and modulus distributions.

ref[1]	method[2]	species	B M T[3]	gross section		interior ($x = 0$)		exterior ($x = 1$)		proposed relationship
				V_f	E_L (GPa)	V_f	E_L (GPa)	V_f	E_L (GPa)	
1, 2	IA	general	nr	0.40	-	0.20	-	0.60	-	$V_f = 0.40x + 0.20$
3	V_f: IA E_L: RoM	*P. edulis*	B	-	9.1	0.09	2.5	0.77	22.6	exponential V_f $E_L = (E_{L,x=0})e^{2.2x}$
			T	-	13.7	0.11	3.8	0.88	33.8	
4	V_f: IA E_L: tens	*P. edulis*	B	0.25	-	0.17	4	0.50	29	exponential V_f and E_L
			M	0.28	-	0.18	6	0.56	30	
			T	0.34	-	0.10	6	0.60	32	
5	IA	*P. edulis*	nr	0.28	-	0.12	-	0.62	-	$V_f = 0.49x^2 + 0.0066x + 0.12$
5	IA	*D. giganteus*	B	0.42	-	0.29	-	0.53	-	$V_f = -0.09x^2 + 0.33x + 0.29$
			M	0.43	-	0.21	-	0.62	-	$V_f = 0.07x^2 + 0.29x + 0.26$
			T	0.43	-	0.19	-	0.60	-	$V_f = -0.12x^2 + 0.51x + 0.21$
6	V_f: SEM E_L: tens	*G. angustifolia*	B	0.26	16.0	0.19	-	0.62	-	$V_f = 0.83x^2 - 0.41x + 0.19$
			M	0.26	14.6	-	-	0.54	-	$V_f = -1.02x^3 + 2.61x^2 - 1.38x + 0.33$
			T	-	13.2	-	-	0.54	-	$V_f = -4.13x^4 + 9.68x^3 - 6.68x^2 + 1.71x - 0.04$
7	tens	*P. edulis*	M	-	-	0.12	4.5	0.54	21	$E_L = 40.13V_f + 0.22$
8	nano	*P. edulis*	nr	-	-	-	6.5	-	13.8	none reported
9	SEM	*P. edulis*	B	0.21	-	0.06	-	0.52	-	$V_f = (0.23x + 0.71)(0.09e^{1.83x})$
			M	0.23	-	0.06	-	0.58	-	$V_f = (0.23x + 0.71)(0.09e^{1.48x})$
			T	0.26	-	0.06	-	0.69	-	$V_f = (0.23x + 0.71)(0.09e^{2.11x})$
10	V_f: SEM E_L: nano	*P. edulis*	nr	-	14.9	0.07	-	0.58	-	none reported
		G. angustifolia	nr	-	19.7	0.16	-	0.60	-	
		B. stenostachya	nr	-	13.8	0.05	-	0.42	-	
11	flex	*P. edulis*	nr	-	8.7	-	2.8	-	15.2	$E_L = 12.43x^{0.43} + 2.78$
12	V_f: SEM E_L: tens	*D. giganteus*	M	-	-	0.38	17.6	0.55	30.7	culm wall divided into thirds
		at $x = 0.5$		-	-	0.45	27.3	-	-	
this study	IA	*P. edulis*	B	0.29	-	0.12	-	0.67	-	$V_f = 1.41x^3 - 1.23x^2 + 0.50x + 0.10$
		P. bambusoides	B	0.32	-	0.14	-	0.65	-	$V_f = 0.96x^3 - 0.91x^2 + 0.57x + 0.10$
		P. nigra	B	0.26	-	0.07	-	0.64	-	$V_f = 0.94x^3 - 0.63x^2 + 0.36x + 0.06$
		P. meyeri	B	0.35	-	0.11	-	0.70	-	$V_f = 0.15x^3 + 0.34x^2 + 0.17x + 0.11$
		B. stenostachya	B	0.35	-	0.24	-	0.64	-	$V_f = 1.75x^3 - 1.98x^2 + 0.75x + 0.20$
		all four Phyllostachys	B	-	-	-	-	-	-	$V_f = 0.86x^3 - 0.61x^2 + 0.40x + 0.09$

x = normalized dimension through culm wall; V_f = fibre volume ratio; E_L = longitudinal tensile modulus of elasticity

[1] references: 1 = Janssen 1981; 2 = Vaessen and Janssen 1997; 3 = Nogata and Takahasi 1995; 4 = Amada et al. 1996; 5 = Ghavami et al. 2003; 6 = Ghavami and Marhinho 2005; 7 = Shao et al. 2010; 8 = Tan et al. 2011; 9 = Dixon and Gibson 2014; 10 = Dixon et al. 2015; 11 = Habibi et al. 2015; 12 = Krause et al. 2016

[2] methods of determining data: IA = image analysis; SEM = scanning electron microscope; RoM = rule of mixtures; tens = tension tests; nano = nanoindentation; flex = flexural tests

[3] locational along height of culm: B = bottom; M = middle; T = top; nr = not reported

457

458

459   Table 2 Mechanical properties bamboo used in this study (COV in parentheses).

species	density at 12% MC, ρ_{12}	moisture content at time of test	compressive strength, f_c	longitudinal shear strength, f_v
	kg/m^3	%	MPa	MPa
P. edulis	896 (0.01)	14.0	48.1 (0.20)	15.1 (0.11)
P. bambusoides	818 (0.04)	14.6	59.3 (0.26)	14.6 (0.22)
P. nigra	907 (0.02)	14.8	45.2 (0.13)	14.6 (0.16)
P. meyeri	840 (0.04)	13.7	55.8 (0.11)	16.4 (0.05)
B. stenostachya	616 (0.03)	13.0	46.0 (0.21)	9.9 (0.11)

460

461

462   Table 3 Summary of experimental results on clipped specimens (COV in parentheses).

species	full-culm control specimens				clipped specimens				
	n	D	t	f_{rC}	n	D	t	f_r/f_{rC}	$\int \dfrac{f_r}{f_{rC}} dx$
		mm	mm	MPa		mm	mm		
P. edulis	33	117 (0.06)	10.1 (0.10)	17.3 (0.18)	13	112 (0.05)	9.5 (0.09)	$4.0x^2 - 4.9x + 2.3$ ($R^2 = 0.82$)	1.18
P. bambusoides	27	95.5 (0.05)	8.2 (0.22)	15.7 (0.21)	14	94.8 (0.06)	8.1 (0.24)	$2.6x^2 - 2.5x + 1.5$ ($R^2 = 0.31$)	1.12
P. nigra	31	93.5 (0.03)	6.7 (0.19)	15.6 (0.14)	16	92.4 (0.01)	6.5 (0.14)	$0.7x^2 - 0.8x + 1.4$ ($R^2 = 0.08$)	1.23
P. meyeri	49	65.3 (0.12)	6.6 (0.10)	20.0 (0.16)	20	65.2 (0.09)	6.4 (0.11)	$2.4x^2 - 1.8x + 1.1$ ($R^2 = 0.59$)	1.00
B. stenostachya	39	77.5 (0.06)	14.5 (0.32)	9.4 (0.13)	17	75.4 (0.06)	14.7 (0.28)	$4.1x^2 - 3.6x + 1.6$ ($R^2 = 0.77$)	1.17

463

464

465 Table 4 Summary of results from specimens having outer layer removed (COV in parentheses).

species	n	D	t	modulus of rupture, f_r		deflection, δ		f_r/δ	
		mm	mm	MPa	p[1]	mm	p[1]	MPa/mm	p[1]
P. bambusoides	10	99.6 (0.01)	6.47 (0.09)	18.1 (0.08)	0.09	1.86 (0.13)	0.00	9.9 (0.14)	0.01
outer layer removed	10	99.8 (0.01)	0.92*t* (0.04)	19.7 (0.12)		2.30 (0.16)		8.4 (0.08)	
P. nigra	10	96.0 (0.01)	8.44 (0.03)	26.4 (0.16)	0.75	2.10 (0.09)	0.59	12.6 (0.15)	0.99
outer layer removed	9	95.8 (0.01)	0.95*t* (0.02)	26.0 (0.06)		2.06 (0.06)		12.6 (0.06)	
P. meyeri	4	62.8 (0.00)	6.58 (0.02)	22.5 (0.08)	0.22	0.95 (0.20)	0.06	25.0 (0.33)	0.09
outer layer removed	5	62.9 (0.01)	0.95*t* (0.02)	21.0 (0.07)		1.21 (0.14)		17.6 (0.14)	
B. stenostachya	7	71.7 (0.02)	15.00 (0.03)	13.8 (0.10)	0.86	1.59 (0.22)	0.10	9.3 (0.30)	0.13
outer layer removed	9	72.2 (0.02)	0.95*t* (0.04)	14.0 (0.09)		1.91 (0.18)		7.6 (0.17)	
[1] p-values indicate the probability that there is no statistical difference between the compared samples									

466
467
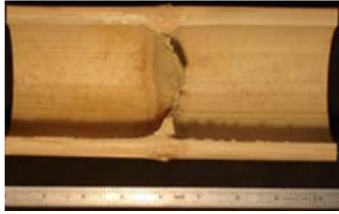
| a) longitudinal section of bamboo culm showing portions of internodes to either side of node | b) cross section of culm near node diaphragm | c) section through culm wall | d) vascular bundle |
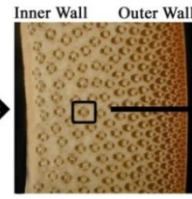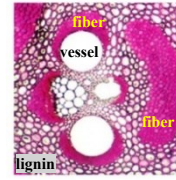
468 Figure 1 Anatomy of bamboo culm showing functionally graded distribution of fibre in culm wall
469 [adapted from Richard 2013].
470

The plot contains the following equations:

$V_f = (0.23x + 0.71)(0.09e^{1.83x})$ [Dixon and Gibson 2014]

$E_f/E_m = 19.4$ [Janssen 1981, 2000]

$E_L = V_f E_f + (1-V_f)E_m$ [rule of mixtures; Eq. 1]

$E_T = E_m(1 + 2nV_f)/(1-nV_f)$ [Halpin-Tsai; Eq. 3]

Axis labels: $V_f/V_{f,average}$, $E_L/E_{L,average}$, $E_T/E_{T,average}$, fibre volume ratio, V_f

x-axis: ←inner   normalised culm wall thickness, x outer →

471

472
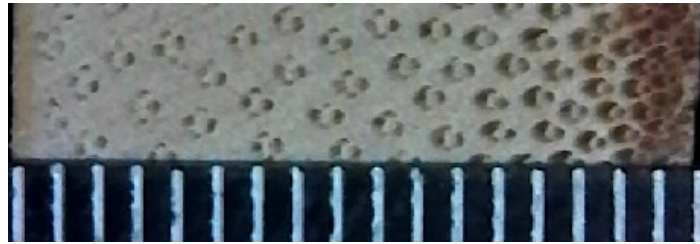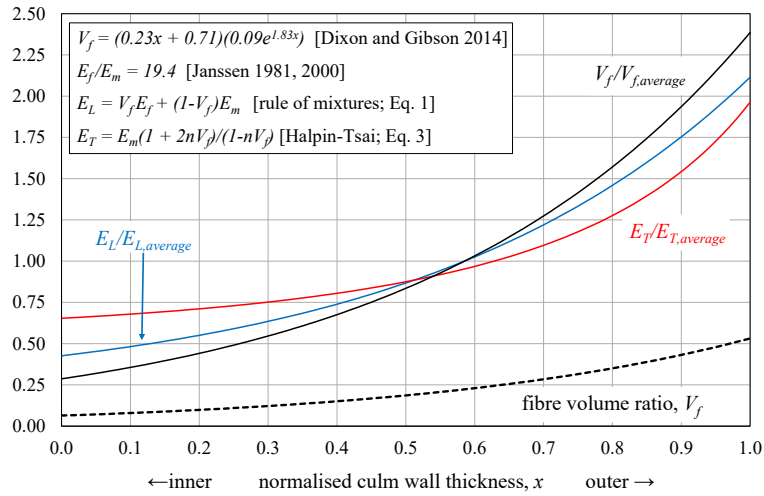
473   Figure 2 Distribution of fibres and modulus through culm wall based on rule of mixtures.

474
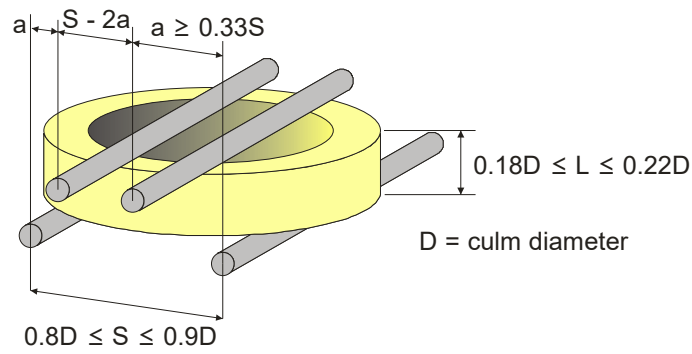
a) test set-up schematic and dimensions
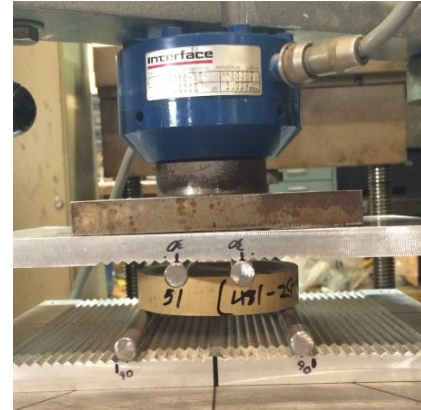
b) test being conducted in universal test machine (shown: 100 mm diameter culm tested over 80 mm span with 25 mm shear span)

475   Figure 3 Flat ring flexure test.

476

477

478
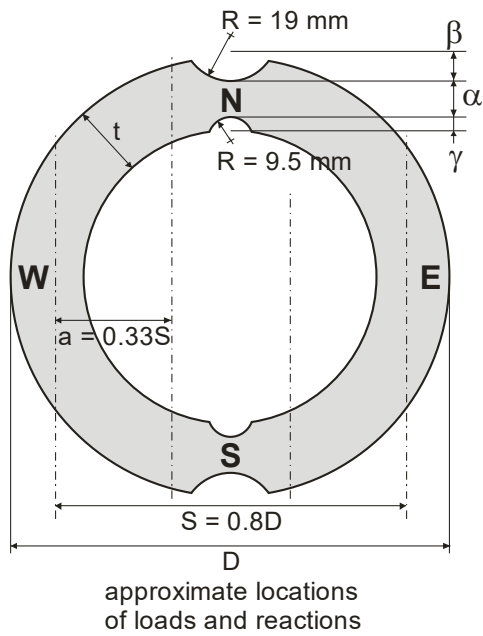
a) test specimen schematic and dimensions   b) specimen machining (shown: $\beta = 0$, α = 0.20t and therefore, $\gamma = 0.80t$)

479   Figure 4 Flat ring flexure specimen.

480
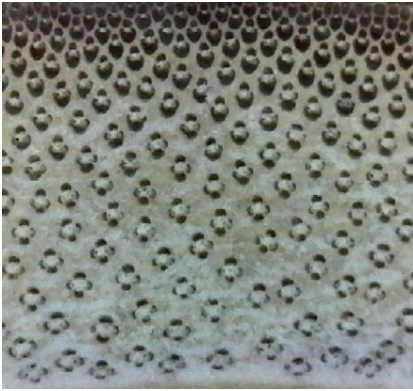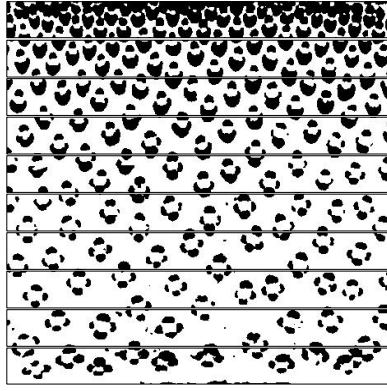
| a) image of culm wall | b) MatLab pixel map of fibres divided into ten layers | c) fibre volume distribution for 28 *P edulis* samples, Black line corresponds to image in figures a) and b) |
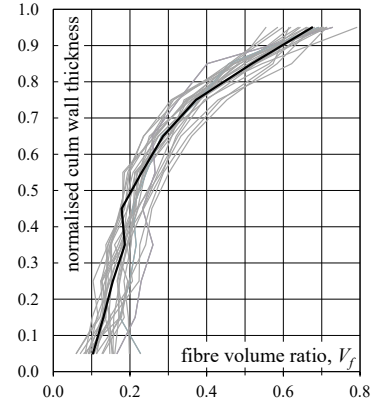
481   Figure 5 Example of digital image analysis of culm wall (*P.edulis* sample shown)

482

483

484

485
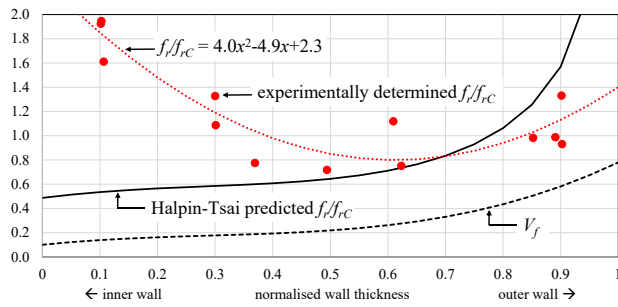
a) *P. edulis*
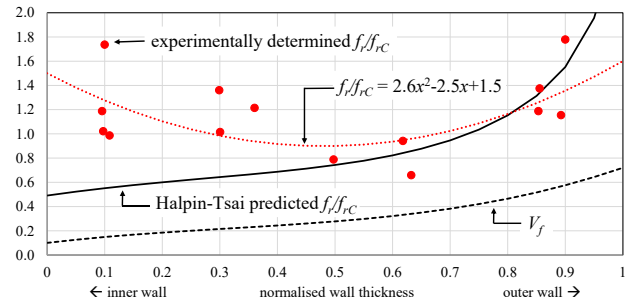
b) *P. bambusoides*
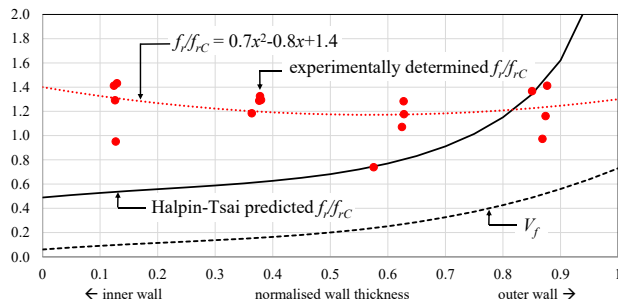
c) *P. nigra*
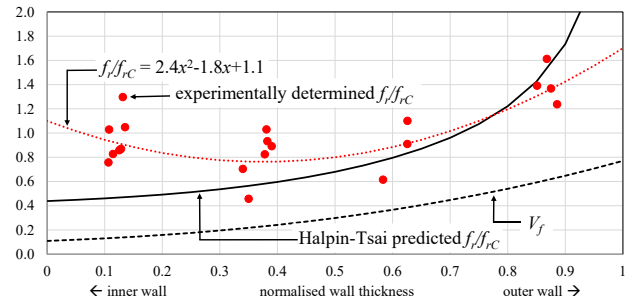
d) *P. meyeri*
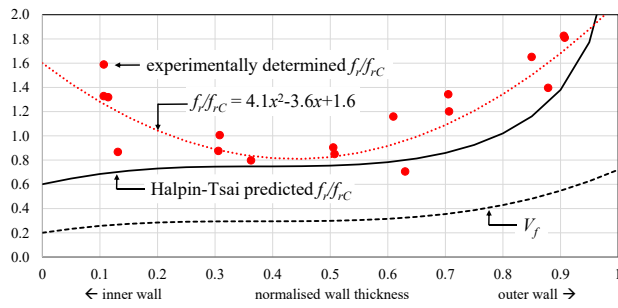
e) *B. stenostachya*

486   Figure 6 Variation of modulus of normalised rupture through culm wall section.
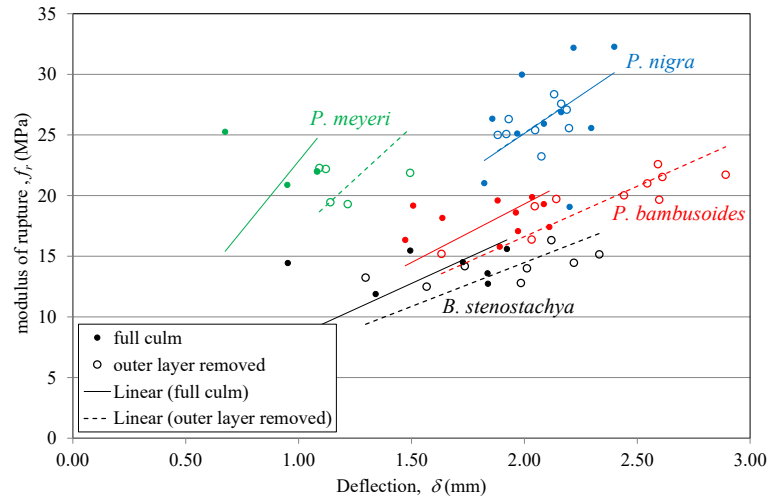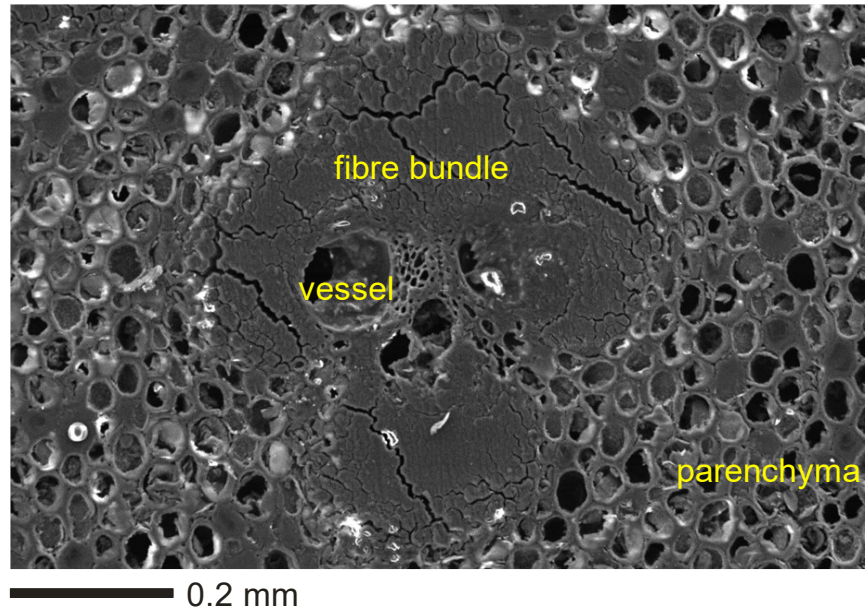
487

Figure 7 Comparison of full-culm specimens and those having only outer layer removed.
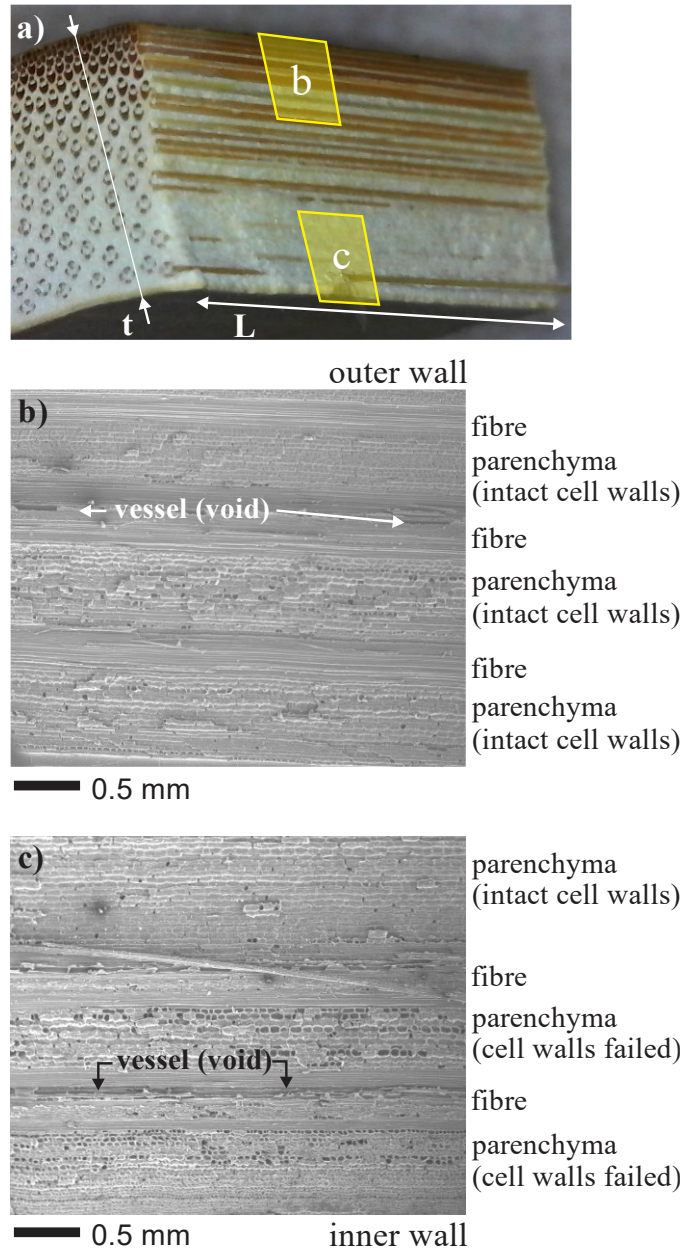
0.2 mm

Figure 8 SEM image of *P.edulis* vascular bundle

491
492
493

a)

outer wall

b)

fibre
parenchyma
(intact cell walls)
fibre
parenchyma
(intact cell walls)
fibre
parenchyma
(intact cell walls)

vessel (void)

0.5 mm

c)

parenchyma
(intact cell walls)

fibre
parenchyma
(cell walls failed)
fibre
parenchyma
(cell walls failed)

vessel (void)
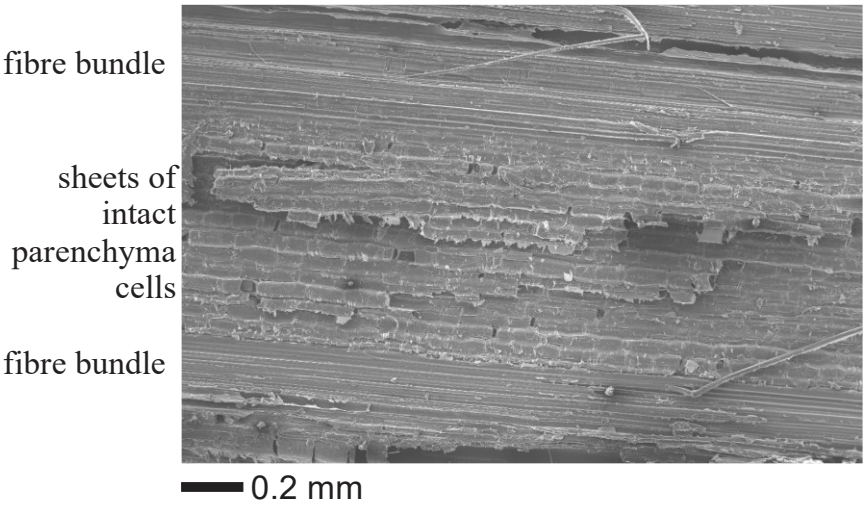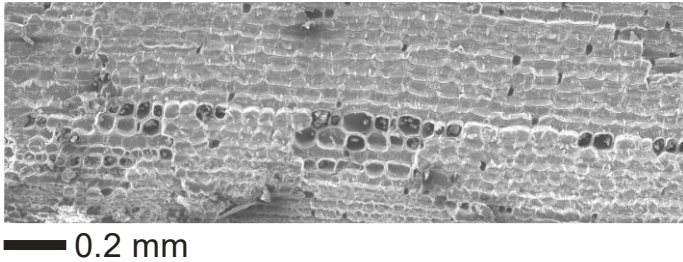
0.5 mm   inner wall

494
495
496
497
498

Figure 9 Detail of culm wall images of *P. edulis* specimen
(note that images in parts b and c are not the same specimen as shown in a)

fibre bundle

sheets of
intact
parenchyma
cells

fibre bundle

0.2 mm

a) parenchyma between two fibre bundles near outer culm wall

0.2 mm

b) parenchyma near inner culm wall

Figure 10 SEM images of *P. edulis* parenchyma.

500
501

50 μm

10 μm

a) near inner culm wall   b) middle of culm wall   c) near outer culm wall
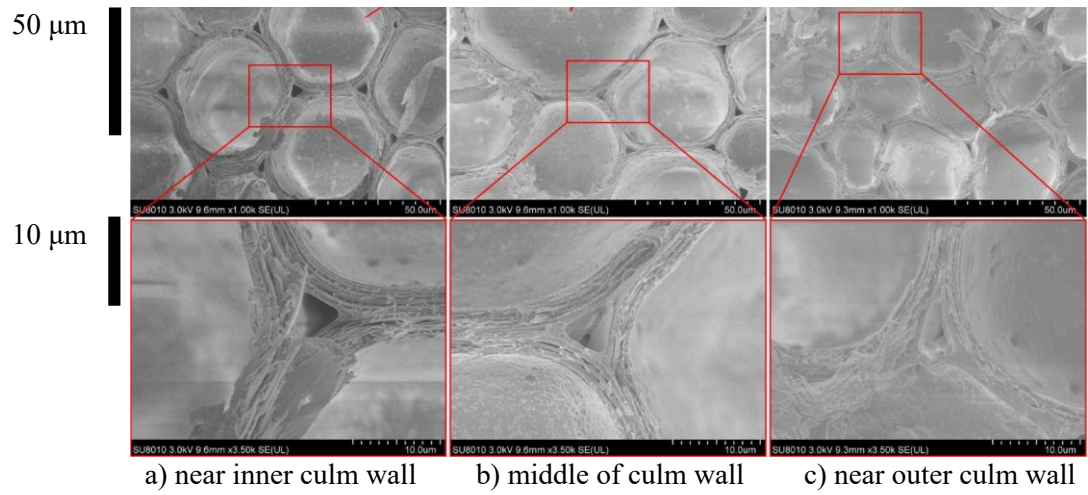
502   Figure 11 SEM images of parenchyma cell wall interstices (Zeng et al. 2019)
503